



Computation by Ensemble Synchronization in Recurrent Networks with Synaptic Depression

ALEX LOEBEL AND MISHA TSODYKS

Department of Neurobiology, Weizmann Institute of Science, Rehovot 76100, Israel

misha@weizmann.ac.il

Received July 23, 2001; Revised May 2, 2002; Accepted May 16, 2002

Action Editor: Carson C. Chow

Abstract. While computation by ensemble synchronization is considered to be a robust and efficient way for information processing in the cortex (C. Von der Malsburg and W. Schneider (1986) *bc* 54: 29–40; W. Singer (1994) *Inter. Rev. Neuro.* 37: 153–183; J.J. Hopfield (1995) *Nature* 376: 33–36; E. Vaadia et al. (1995) *Nature* 373: 515–518), the neuronal mechanisms that might be used to achieve it are yet uncovered. Here we analyze a neural network model in which the computations are performed by near coincident firing of neurons in response to external inputs. This near coincident firing is enabled by activity dependent depression of inter-neuron connections. We analyze the network behavior by using a mean-field approximation, which allows predicting the network response to various inputs. We demonstrate that the network is very sensible to temporal aspects of the inputs. In particular, periodically applied inputs of increasing frequency result in different response profiles. Moreover, applying combinations of different stimuli lead to a complex response, which cannot be easily predicted from responses to individual components. These results demonstrate that networks with synaptic depression can perform complex computations on time-dependent inputs utilizing the ability to generate temporally synchronous firing of single neurons.

Keywords: mean field, population spike (PS), recurrent network, synaptic depression

1. Introduction

Computations in neo-cortical circuits are traditionally believed to be carried out by selective increase or decrease of firing rates of single neurons. A classical example of this phenomenon is the orientation dependent firing rate of neurons in the primary visual cortex of mammals, measured as a number of spikes emitted in a certain time window after the presentation of the stimulus (Hubel and Wiesel, 1962). This description implicitly assumes that timing of single spikes, either absolute or relative to spikes of other neurons, does not carry information relevant to the computation in question. However, there are a growing number of observations, which indicate that information can in fact be represented in the temporal domain (Murphy et al., 1985;

Gray et al., 1989; Vaadia and Aertsen, 1992). For example, in the auditory cortex neurons have a tendency to respond in a strongly transient manner, often emitting just one spike on average per presentation of the stimulus (Phillips and Sark, 1991). Clearly, for these neurons the notion of a firing rate defined as a spike count does not exist at all. One is therefore forced to think about the computational strategies, which would utilize the timing of single spikes. The simplest such strategy involves generating a synchronous, near coincident firing of a group of neurons, which would indicate the presence of a certain feature in the sensory stimulus. Indeed, several observations of a near coincident firing of neurons were recently reported in the literature (Riehle et al., 1997; Abeles and Prut, 1996; Villa et al., 1999). In order to carry information about external stimuli, the

synchronization of spikes has to be stimulus selective and robust to noise. In a previous numerical study, we demonstrated that selective and robust synchronization is observed in a recurrent network in which excitatory neurons are randomly interconnected with depressing synapses (Tsodyks et al., 2000). In particular, it was shown that the network could generate a ‘Population Spike’ (PS), characterized by a near coincident firing of neurons, each firing only one or two spikes, as a response to an external excitatory input pulses in an all-or-none fashion. Moreover, for a given amplitude of the pulses, the response was selective to the identity of the neurons targeted, i.e. despite of the randomness, the network exhibited the selectivity to external inputs, thus enabling it to perform useful computations.

In the current work, we analyze the computational ability of the recurrent network in more detail. To this end, we formulate a simplified description of the network behavior by using time coarse-grained equations (Wilson and Cowan, 1972), which include the effects of short-term synaptic plasticity. While in this approach the activity of the neurons is described by analog variables (rates), synchronous firing of neurons is expressed in a sharp increase in rates across the network. Analyzing the time coarse-grained equations (which we’ll refer to as the Rate model) by applying a mean-field formalism, allowed us to gain a deeper understanding of the dynamic mechanisms of network synchronization and quantitatively analyze the computations the network can perform on its inputs. We also considered different types of inputs, and analyzed the network responses to each of them separately, as well as the interesting effects of nonlinear interference observed when several inputs were presented simultaneously. Finally, we compare the results of the analysis to some of the properties of neuronal responses in the auditory cortex to different types of stimuli.

2. Methods

2.1. Rate Based Network

We considered a fully connected recurrent network of N excitatory units, with depressing synaptic dynamics. Only excitatory units were included, since the main features of the network dynamics and responses to external stimuli do not depend on the presence of an inhibitory part, and the analytical analysis is much simplified. The system of equations, which is used to describe the network, is based on Rate model of Wilson and

Cowan (1972) and Grossberg (1988), in which short-term synaptic plasticity was introduced (Tsodyks et al., 1998; also see 2.2). In short, each unit is represented by a firing rate variable, E_i . The input to the units is combined of two terms: the first term represents local synaptic connections between the different parts of the network, with a depressing dynamics. The second term is an external input, which represents both afferent feed-forward (sensory) inputs, and feedback inputs from other brain areas, innervating the network with constant amplitudes, distributed across a chosen interval of values. In the following, we chose the distribution to be uniform. If the parameters that characterize the synaptic connections (τ_{rec} —the synapse recovery time from depression, U —the utilization of the synaptic recovered resources at a spike, J —maximum efficacy of a connection) are taken to be the same for all connections, the system of rate equations has the following form:

$$\tau \dot{E}_i = -E_i + \left[\frac{J}{N} \sum_{j=1}^N E_j x_j + e_i \right]^+ \quad (1)$$

with the complimentary equation for the time evolution of the synaptic depression factor:

$$\dot{x}_i = \frac{1 - x_i}{\tau_{rec}} - U x_i E_i \quad (2)$$

where $i = 1..N$ and (e_1, \dots, e_N) are the external inputs to the units, labeled in increasing order. x_i defines the depression rate of connections originating from neuron i . The time constant τ determines how quickly the firing rates change following the synaptic input. As found in Treves (1993), the speed of the change is controlled by synaptic conductance, i.e. the corresponding time constant is of the order of a ms. The rectifying term on the right hand side of Eq. (1) has the following functional form:

$$[z]^+ = \begin{cases} 0 & z \leq 0 \\ z & 0 < z \leq \Theta \\ \Theta & \Theta < z \end{cases}$$

where Θ is the saturation value for the firing rate of a unit. Its dimensions, as for the e_i ’s and E_i ’s, are of Hz.

In simulations, we introduced a refractory period, τ_{ref} , into Eq. (1), which enabled us to control the amplitudes of the PS, without affecting the analytical analysis and the numerical results. Following Wilson and

Cowan (1972) we used the following form for Eq. (1):

$$\tau \dot{E}_i = -E_i + (1 - \tau_{ref} E_i) \left[\frac{J}{N} \sum_{j=1}^N E_j x_j + e_i \right]^+ \quad (1a)$$

In the subsequent simulations and numerical analysis, the following values of the parameters were chosen:

$$\begin{aligned} \tau &= 1 \text{ ms}, \quad \tau_{ref} = 3 \text{ ms}, \quad \tau_{rec} = 800 \text{ ms}, \\ e_1 &= -10 \text{ Hz}, \quad e_N = 10 \text{ Hz}, \quad N = 100, \\ U &= 0.5, \quad \Theta = 300 \text{ Hz}. \end{aligned}$$

The values for τ_{rec} and U were based on experimental data (Tsodyks and Markram, 1997), while those of e_1 and e_N were chosen by setting the networks' mean spontaneous activity to a few Hz, representing in vivo findings (Abeles, 1991).

2.2. Integrate and Fire Network

In the simulations we conducted to verify that the results obtained from the rate based network remain valid for the original integrate and fire (I&F) network, in which PS were first observed (Tsodyks et al., 2000), we considered a network of 400 I&F excitatory units (Tuckwell, 1988), that were randomly connected by depressing synapses with probability of connection of 0.1 for any given two units. The equation that governs the evolution in time of the membrane potential (V) of each unit has the following form:

$$\tau_{mem} \dot{V} = -V + I_{syn} + I_b \quad (3)$$

where τ_{mem} is the membrane time constant, I_{syn} is the synaptic input, and I_b stands for the nonspecific background input provided by distant brain areas. The threshold value was chosen to be 15 mV, at which a spike was emitted, and the membrane potential was reset to 13.5 mV. A refractory period of 3 ms was used, and I_b had a fixed value for each unit, chosen randomly from a uniform distribution. The synaptic input was modeled by:

$$I_{syn}(t; i) = \sum_j J_{ij} y_j(t) \quad (4)$$

Where J_{ij} represents the maximum efficacy of the synaptic connection from unit j to unit i , and $y_j(t)$ is derived from the short term synaptic plasticity model, which governs the evolution in time of the synaptic

resources:

$$\dot{x} = \frac{z}{\tau_{rec}} - Ux\delta(t - t_{sp}) \quad (5a)$$

$$\dot{y} = -\frac{y}{\tau_{in}} + Ux\delta(t - t_{sp}) \quad (5b)$$

$$\dot{z} = -\frac{z}{\tau_{rec}} + \frac{y}{\tau_{in}} \quad (5c)$$

Here x , y , z represents the resources in their three possible states: the recovered, the active and the inactive state, respectively. When a spike arrives to a synapse, at $t = t_{sp}$, a fraction of the recovered resources (determine by the value of U) is utilized to the active state instantaneously. After a few ms they inactivate, and recover back to the recovered state with a characteristic time constant of the order of a second (Abbott et al., 1997; Tsodyks et al., 1998).

In simulations, the values of the parameters were:

$$\begin{aligned} \tau_{mem} &= 30 \text{ ms}, \quad \tau_{in} = 3 \text{ ms}, \\ \tau_{rec} &= 800 \pm 400 \text{ ms}, \quad U = 0.5 \pm 0.25. \end{aligned}$$

τ_{mem} and τ_{in} were constant for all the units, τ_{rec} and U were chosen from a normal distribution of mean \pm SD (with boundaries cut-offs, to simulate biological constraints, $0.1 < U < 0.9$, $\tau_{rec} \geq 5$ ms), and the background input (I_b) was uniformly distributed around the mean value of 14.7 mV, with a range of 0.4 mV. The values of J_{ij} are mentioned where appropriate. Simulations were performed using Euler method, with a time step of 0.1 ms. Reducing the time step down to 0.002 ms did not lead to different results. Also introducing a small (1 ms) finite rising time of synaptic inputs did not result in any significant changes in the solutions.

3. Results

3.1. Steady States and Stability

We started the investigation of the rate based network by looking for its steady state solutions, in which the firing rate and the depression variables of the units are constant in time. Equations (1) and (2) lead to the following steady state equations for the rates ($\{E_i\}$) and the depression factors ($\{x_i\}$):

$$E_i^* = [JH^* + e_i]^+ \quad (6a)$$

$$x_i^* = \frac{1}{1 + \tau_{rec} U E_i^*} \quad (6b)$$

$$H^* = \frac{1}{N} \sum_{j=1}^N E_j^* x_j^* \quad (6c)$$

We have introduced the network mean-field variable (H), which defines the common synaptic input received by every unit in the network:

$$H = \frac{1}{N} \sum_{j=1}^N E_j x_j \quad (7)$$

The mean-field variable allows one to reduce the analysis of the system from $2N$ equations of the form of Eqs. (6a and b), to the investigation of one equation of the form of Eq. (6c). Expressing the right hand side of Eq. (6c) in terms of H yields:

$$H = g(JH) \quad (8)$$

$$g(JH) = \frac{1}{N} \sum_{j=1}^N \frac{[JH + e_j]^+}{1 + \tau_{rec} U [JH + e_j]^+} \quad (9)$$

For a large number of neurons, Eq. (9) can be transformed into an integral that has an analytical form (Appendix A). Solving (8) yields H^* , and planting it in Eqs. (6a and b) gives us the steady state values of the network variables: E^* and x^* .

To determine the stability of the steady state, we used the fast-slow variables method to derive an approximated dynamical equation of the mean-field variable, H , in the vicinity of the fixed points (Appendix A). Near the steady state, it has the following form:

$$\tau \dot{H} = -H + \bar{g}(JH; H^*) \quad (10)$$

$$\bar{g}(JH; H^*) = \frac{1}{N} \sum_{j=1}^N \frac{[JH + e_j]^+}{1 + \tau_{rec} U [JH^* + e_j]^+} \quad (11)$$

If the derivative on the right hand side of Eq. (10), at H^* , is smaller than 0, the steady state is stable, otherwise the steady state is unstable. In Fig. 2 the curves of H , $g(JH)$ & $\bar{g}(JH; H^*)$ are shown for some chosen value of J . The point where all three curves intersect is the steady state of the system (in the case of Fig. 2, a stable one). Another intersection point between the curves of H & $\bar{g}(JH; H^*)$ can also be present with stability nature always opposed to the one of the networks' steady state (Fig. 2). As J increases to a critical value, J_c , the two intersection points collapse and the steady state becomes unstable, resulting in spontaneous generation of Population Spikes (Fig. 1) (The conditions for the transition are presented in Appendix B). PS is the way instability is expressed in the network, explained by the following argument: divergence of the activity of the units in the network is followed by a quick decrease in the strength of the synapses, due to the negative feedback the rate variables have on the synaptic depression

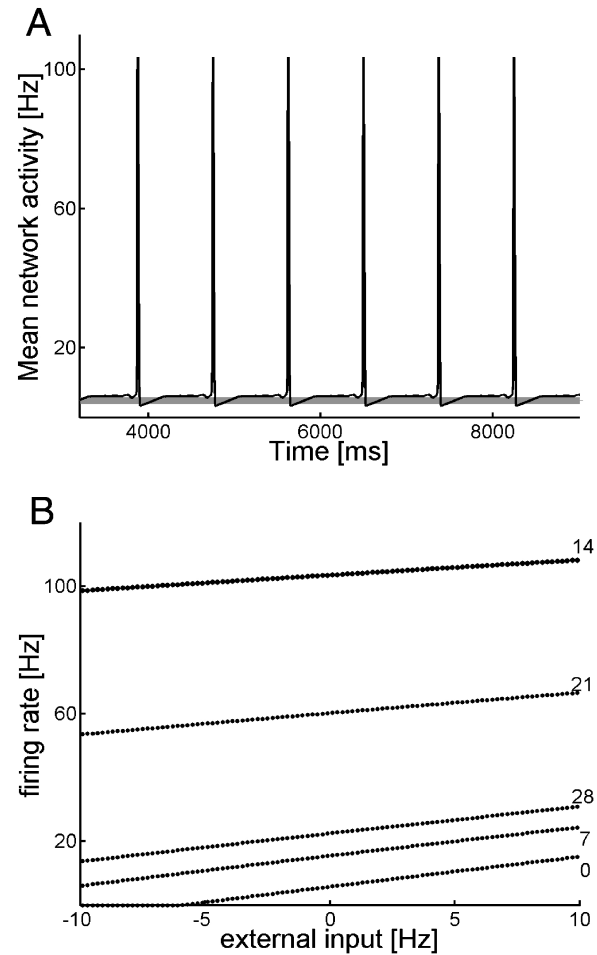


Figure 1. **A:** Results of simulations for synaptic efficacy below the critical value (bold grey line, $J = 3.6 < J_c$) and above the critical value (black line, $J = 4.4 > J_c$). The y-axis represents the average Disk network activity ($\frac{1}{N} \sum_{i=1}^N E_i(t)$). While at stable state of the network followed only a fraction of the units is active (those with $e_i > -JH^*$, see Eq. (6a)), during the PSs all the units are synchronously active for a very short time interval (~ 20 ms). Furthermore, by integrating the area under the curve at the PS, we calculated that only one to two spikes are added to the overall firing pattern of the units at each of the PSs, emphasizing the ensemble recruitment effect. **B:** Firing rate of the units, arranged by their external inputs, at different times near a PS. The numbers near each line are in ms, '0' represents the onset of the PS, '14' its peak.

variables (Eq. (2)). This synaptic weakening uncouples the units, and the network returns to an asynchronous level of activity, in which the synapses strength slowly recovers (time scale of τ_{rec}), the units couple again, and the PS cycle is complete. For $J > J_c$, the frequency of the PSs is an increasing function of J , while their amplitudes slowly decreases. We also found that the asynchronous activity of the network (the activity in

the stable state, for $J < J_c$, or the activity in between PSs for $J > J_c$ rises smoothly with J , and shows no discontinuities. Furthermore, we wish to emphasize that in PSs, a unit produces only 1.1–1.6 spikes per PS (Tsodyks et al., 2000), suggesting that it is the correlated temporal grouping of firing of the units that determines the network spontaneous PS activity, and is the main feature of the instability.

3.2. Response to External Stimuli

In order to study the computational capabilities of the network, we considered its response to various types of stimuli. Before the stimuli were presented, the network was at a state of low asynchronous spontaneous activity ($J < J_c$).

3.2.1. Response to a Single Pulse. We first considered the response of the network to a single pulse of excitation, which leads to instantaneous elevation of the activities of the units ($\forall i : E_i \rightarrow E_i + \Delta E_i$). For an arbitrary distribution of input amplitudes, the response can be calculated from the curves of the two gain functions (Eqs. (9) and (11)) as shown in Fig. 2: While a network is in a stable state, the second intersection point determines the boundary of the basin of

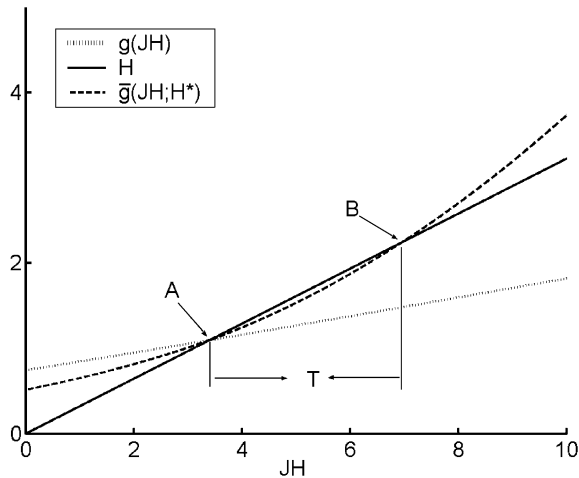


Figure 2. An example for the curves of H , $g(JH)$ & $\bar{g}(JH; H^*)$ vs. JH , for $J = 3.1$. The two different intersection points are shown: the stable steady state (A), which is the intersection of all three curves, is the steady state of the network (derived from Eq. (8)), while the second intersection point (B), with an unstable characteristic, defines the boundary of the basin of attraction of the stable steady state: pushed beyond this point, i.e. via some external stimulus, the network activity would diverge, and a PS will occur.

attraction of the stable steady state. By driving the activity of the network beyond this point, the network activity diverges and a PS occurs. From Eq. (7), the change in the meanfield variable due to the inputs is:

$$\Delta H = \frac{1}{N} \sum_{j=1}^N \Delta E_j x_j^* \quad (12)$$

where x_j^* is the depression variable value at the stable steady state (which can be calculated from Eq. (6b)). For any given set $\{\Delta E_j\}$ of inputs, which satisfies $J\Delta H \geq T$ (T being the minimum value needed to cause divergence, Fig. 2), the network activity would diverge, and a PS is predicted:

$$\text{Network output} = \begin{cases} \text{PS} & \text{if } \frac{J}{N} \sum_{j=1}^N \Delta E_j x_j^* > T \\ \text{no PS} & \text{Otherwise} \end{cases} \quad (13)$$

It is interesting to note the resemblance of (13) to a Perceptron (Rosenblatt, 1962): In our case, T represents the Perceptron threshold, the set $\{\Delta E_j\}$ is the input to the Perceptron input layer, the set $\{x_j^*\}$ plays the role of the synaptic weights, and the 1 or 0 output of the Perceptron corresponds to whether the network emits a PS or not. However, unlike the Perceptron, in our case the network itself plays the dual role of the input and output layer, and for the same set of inputs, the networks' output depends on the feedback from other brain areas, which determines the distribution of $\{x_j^*\}$.

In simulations we conducted in order to verify the validity of this analysis, we introduced the network with sets of sharp (width of 1 ms) inputs $\{\Delta E_j\}$, randomly chosen from a uniform distribution at each simulation, such that $0.98 T \leq J\Delta H \leq 1.02 T$. At only 12 trials, out of 200 (6%), the network response was not as predicted (either emitting a PS when $J\Delta H < T$, or silent when $J\Delta H > T$) (Fig. 3). This result was confirmed over different types of input distributions, i.e. giving a constant input to only 10 units, which were grouped by their similar stable state firing rate, such that:

$$\Delta H = \frac{1}{N} \sum_{j=1}^{10} \Delta E x_j^* \quad (14)$$

3.2.2. Response to Tonic Stimulus. The motivation for considering this kind of stimulus came from

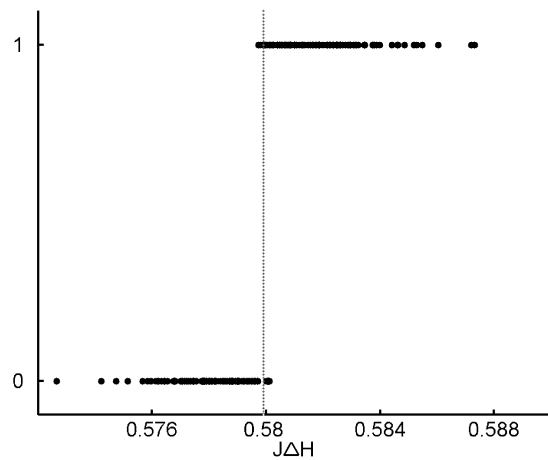


Figure 3. Selectivity of the networks' response to distributed sharp inputs. Each unit receives a sharp pulse with amplitude randomly chosen from a uniform distribution with boundary values of $[0.9\Omega, 1.1\Omega]$. $\Omega = \frac{NT}{J \sum_{j=1}^N x_j^*}$ is the minimal amplitude needed to drive the network to PS, if equally given to the units across the network. The y-axis '1' & '0' correspond to whether the network responded to the sharp pulse with a PS, or without, respectively. The vertical line marks the point where $J\Delta H = T$. $J = 3.6$.

experiments on the primary auditory cortex, which demonstrated that neurons responded in a transient manner to tonic sounds (see e.g., deCharms and Merzenich, 1996; Heil, 1997). A typical response of our network to constant excitatory input, introduced by a prolonged increase to the external inputs ($\forall i : e_i \rightarrow e_i + \Delta e$) is shown in Fig. 4a (the theoretical analysis is presented in Appendix C): If the stimulus amplitude is above a certain threshold (Appendix C), one onset PS occurs, after which the network recovers into a new stable state, with higher average activity. Figure 4b shows the corresponding amplitudes of the average activity of the new stable state and that of the onset response, as a function of the amplitude of the stimulus: while the amplitude of the new stable state is a linear function of the input, the onset response shows a discontinuous jump at the threshold value, after which there is only a small change to its amplitude as a function of the input. Looking for a temporal dependency, we found that information about the amplitude of the tonic stimulus also resides in the time delay to the onset response: the closer the stimulus amplitude is to the threshold, the longer it takes the network to respond (Fig. 4c).

3.2.3. Response to Consecutive Sharp Pulses. Proceeding to a more complex scheme of stimuli, we

studied the response of the network to a train of sharp stimuli of various frequencies. All the units received excitatory pulse inputs of the same amplitude:

$$\Delta E = a\Delta E_{\min} \quad (15)$$

where ΔE_{\min} is the minimal amplitude of the stimulus needed for a PS response. We considered super-threshold amplitude ($a = 1.5$), so that each of the pulses was capable to provoke a PS, when individually stimulating the network. At low frequencies the network's PS followed precisely the timing of the stimulus phases. As the frequency increased, the network ability to follow the different phases with a PS response decreased, till a cut off frequency, above which only the onset PS was observed (Fig. 5). The cut-off frequency exhibits a counter intuitive non-monotonic dependency on the amplitude of the input. In particular, this implies the existence of optimal amplitude, at which the cut-off frequency is maximal (Fig. 6).

3.2.4. Response to Wide Periodic Stimuli. Here, we presented the network with a periodic excitatory input of square shape. A typical response is shown in Fig. 7. For low frequencies of the stimulus, the network responded to each cycle with a strong onset PS, followed by an elevated activity, till the end of the cycle. While the elevated response was only dependent on the amplitude of the input, not its frequency, the onset response weakened as the frequency increased (compare the network response to consecutive sharp pulses). In other words, for given amplitude of a stimulus, the information about its frequency is coded in the amplitude of the transient response.

3.2.5. Complex vs. Simple Stimuli. It was observed that a response of a neuron in the primary auditory cortex to complex sounds couldn't be easily predicted from its response to the components, which constitute the sounds. For example, superimposing a tone with a neurons' preferred frequency to a modulated noise, can paradoxically shut down the neuron response to the otherwise effective noisy stimulus (Nelken et al., 1999). The scheme we used here was as follows: a network was presented with a train of sharp stimuli (as in 3.2.3) with a frequency below the cut-off value. After a while, a tonic stimulus was added, resulting in the interference between the two types of inputs. We found that as the amplitude of the tone increased, the amplitudes of the PS responses to the sharp pulses decreased gradually, until

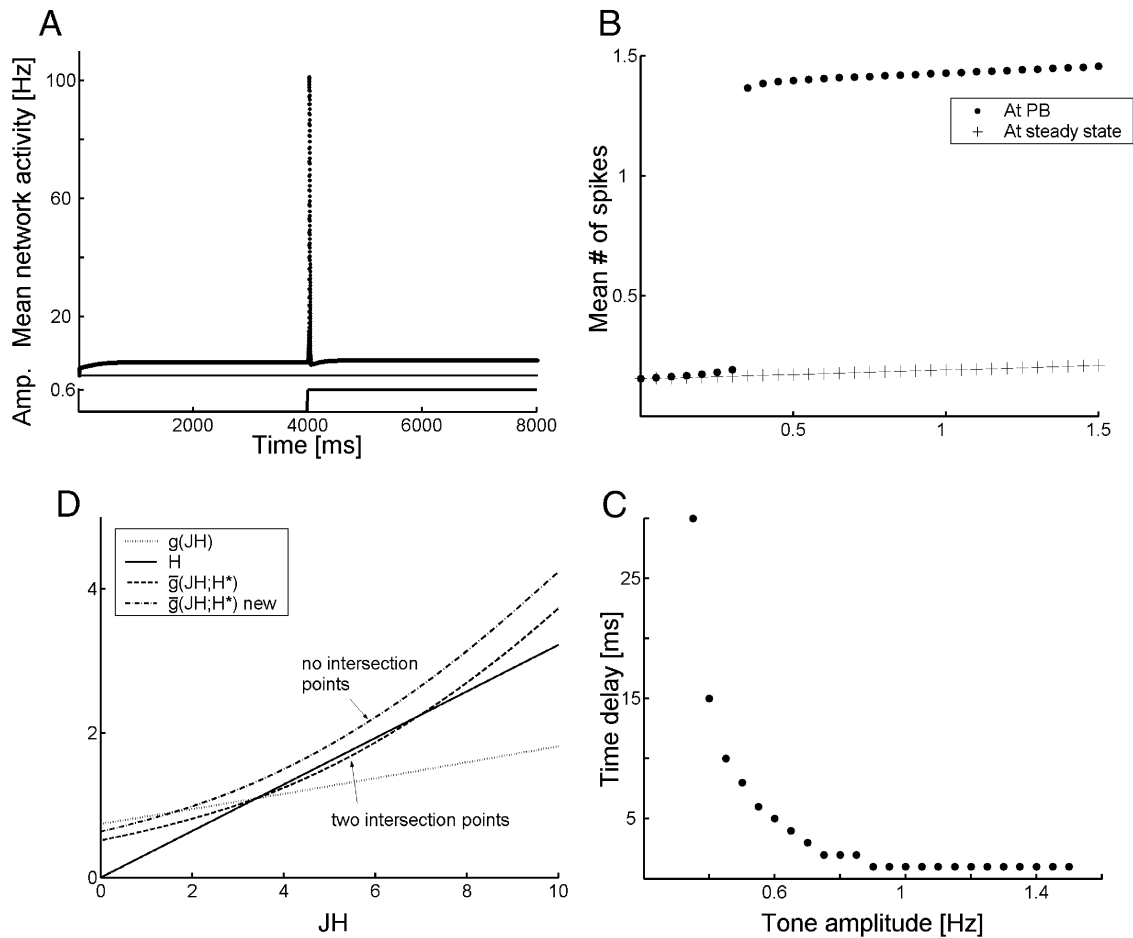


Figure 4. Response of the network to tonic excitation. **A:** Introducing the network with a tonic stimulus of sufficiently strong amplitude results in an onset response after some short delay (not seen on this time scale resolution), after which the network recovers to a new stable steady state. $J = 3.2$, $\Delta e = 0.6$ Hz. **B:** By integrating the area under the curve in (A), with a width of the PS around its peak, one can calculate the network amplitude of the onset response in terms of number of spikes per neuron, emitted at the PS (filled dots). The same was done to calculate the new stable steady state value (with the same integration time window), to which the network recovers after the onset response (+ sign). While the new stable steady state shows linear relation to the tone amplitude, the onset response shows a discontinuous jump at a certain value, at which the first PS appears. **C:** Temporal delay of the onset response of the network vs. tone amplitude. **D:** A graphical view on the numerical solution of Eq. (5) and of the steady state solutions of Eqs. (7) and (C2), explaining the possible divergent response of the network to an increase in the external inputs (the $\{e_i\}$). This is the same plot of the curves of the gain functions, as in Fig. 2, with the supplement of the curve of $\bar{g}(JH + \Delta e; H^*)$. As the amplitude of the external inputs increases, the curve of $\bar{g}(JH + \Delta e; H^*)$ moves away from the curve of H , until no contact points exist. At that moment, the network would diverge, resulting in a PS.

full suppression was observed (Fig. 8). For values of the synaptic efficacy closer to J_c (from below), higher amplitudes of the tonic input were needed in order to suppress the bursting response. Furthermore, for a fixed chosen value of J , the higher the frequency of the sharp stimuli, the lower the tone amplitude needed to suppress it, i.e. the reduced PS amplitude response to the sharp stimulus convey no information about the tone amplitude.

3.3. Comparison to the Integrate and Fire Model

The mathematical formulation presented above is a rate based description of a network, simulated in Tsodyks et al. (2000), with only the excitatory part included (the original work was done on an I&F network of excitatory and inhibitory units). In this part we turned our attention back to the I&F model, to check if it could mimic the principle results that were derived in

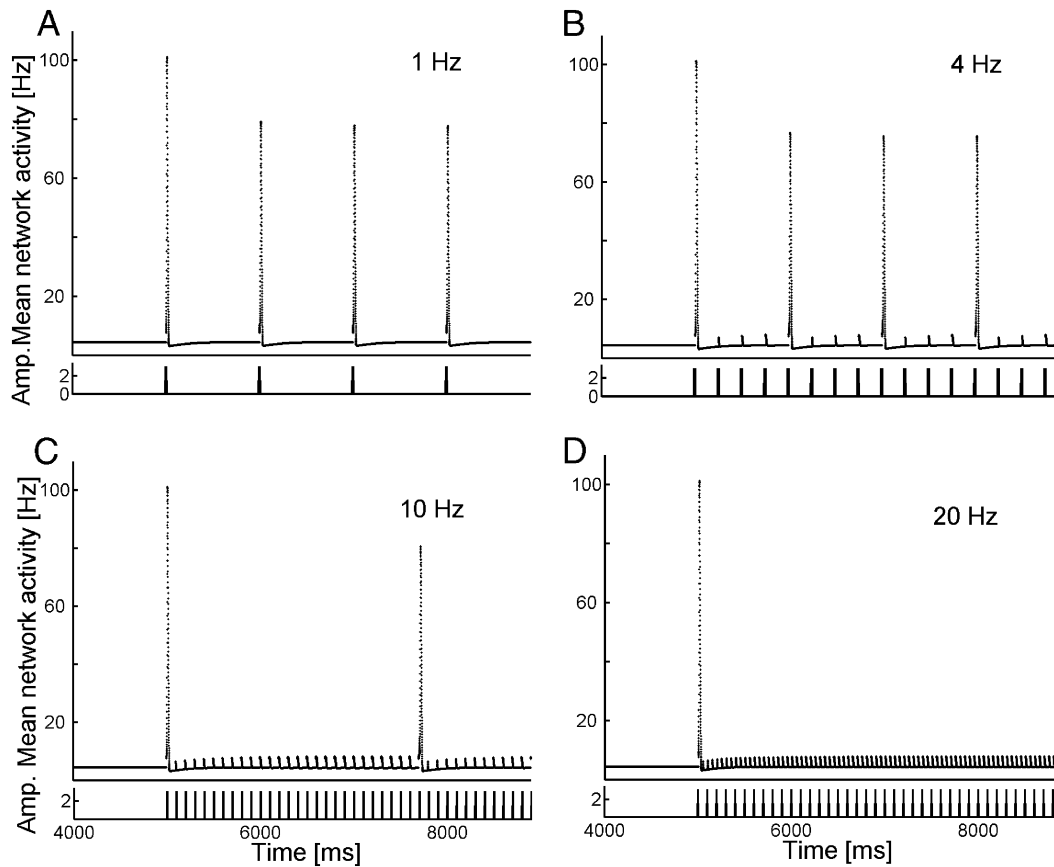


Figure 5. Response of the network to trains of sharp stimuli with increasing frequencies. The y-axis variable is as in Fig. 1. The amplitude of each phase was 3.1 Hz ($1.5 \times \Delta E_{\min}$), the stimulus frequencies in A, B, C and D were 1, 4, 10, 20 Hz, respectively. $J = 3.2$.

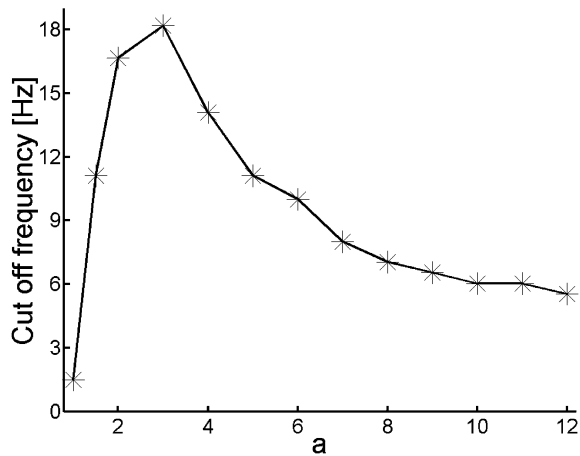


Figure 6. The cut off frequency, which suppresses a PS response to a train of sharp pulses vs. its amplitude. The 'a' (x-axis) is from Eq. (15): $\Delta E = a\Delta E_{\min}$. $\Delta E_{\min} = 2.075$ Hz, for $J = 3.2$.

3.2.1–3.2.5 from the rate based network. In order to stay as close as we can to the formulation of the rate based network described by Eqs. (1) and (2), we built an I&F network comprised only of Excitatory units (described in detailed in 2.2), and presented it with similar input patterns as described in 3.2.1–3.2.5. Even though the results obtained were noisier, the excitatory I&F network exhibited all of the features found for the rate based network: synaptic efficacy dependent switch between stable and spontaneous PS activity; an onset PS followed by an elevated activity in response to a tonic stimulus, and finally, an accurate temporal PS response to a train of sharp excitatory pulses, which can be suppressed by a superimposed tonic stimulus (Fig. 9).

4. Discussion

We presented a detailed analytical and numerical study of recurrent networks with activity-dependent synaptic

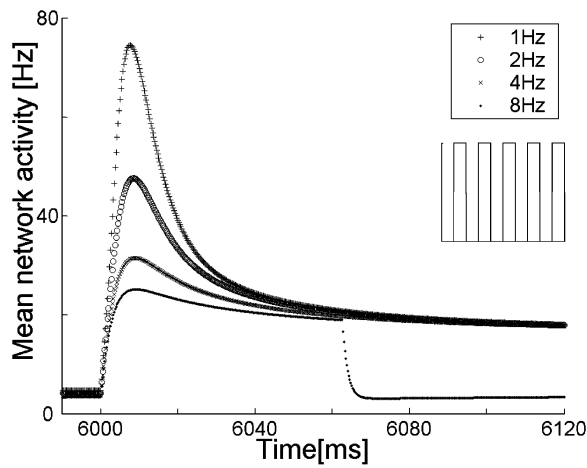


Figure 7. Network response to each phase of an ongoing train of wide inputs. The response can be divided to a transient part, which reflects the network response to the onset of each phase, and a steady part, reflecting the units elevated activity caused by a prolonged increase in the external inputs amplitudes. Increasing the frequency of the input weakens the network transient response, while the elevated activity remains virtually the same. Inset is a caricature of the stimulus given. In the results shown here, tone amplitude was $\Delta e = 5$ Hz. y -axis as in Fig. 1, $J = 3.6$.

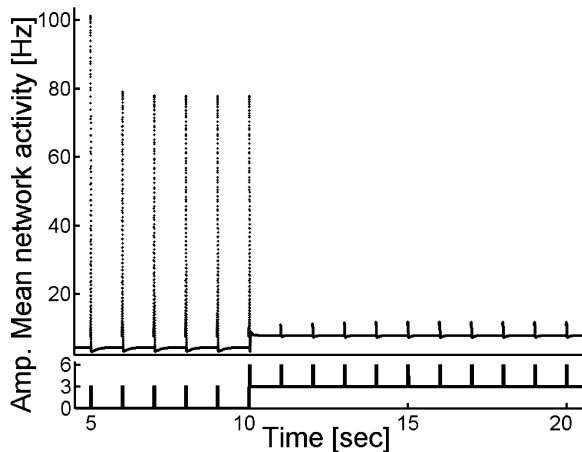


Figure 8. Suppression of a PS response to a train of sharp pulses, as a result of an interference with a tone. Shown here is an example where a phased locked PS response to a train of sharp pulses, with $\Delta E = 1.5 \times \Delta E_{\min}$ (Eq. (15)), and a frequency of 1 Hz, is completely suppressed by an interference with a tone, with an amplitude of 3 Hz. $\Delta E_{\min} = 2.075$ Hz, $J = 3.2$.

depression. The analysis shows that synaptic depression increases the computational ability of these networks. In particular, it enables the network to generate a sharp transient synchronization of neuron's activity for short time periods (population spikes, or PS), either

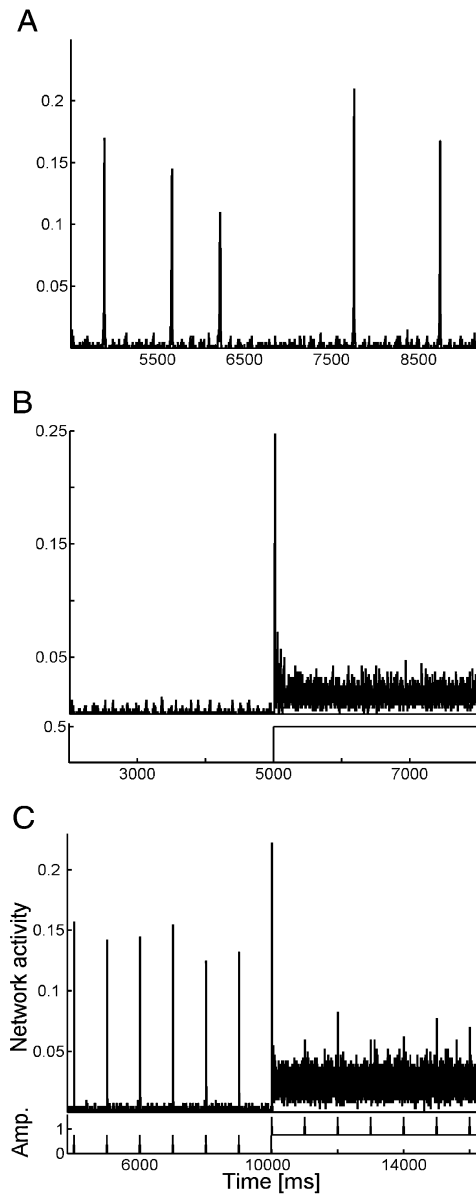


Figure 9. Simulations results of an all-excitatory Integrate & Fire network with depressive synaptic dynamic: **A:** Spontaneous PS activity. Each PS is about 10 ms wide, and $\sim 98\%$ of the units fire in the PS, compared to $\sim 5\%$ during the same period between PSs. $J_{ij} = 1 \pm 0.5$ (Mean \pm SD) mV **B:** Response to a tonic input. A network with no spontaneous PS activity is given a tonic stimulus by raising the background input uniformly across the network. $J_{ij} = 0.8 \pm 0.4$ (Mean \pm SD) mV, amplitude of tone is 0.5 mV. **C:** Suppression of a PS response to a train of sharp pulses, as a result of an interference with a tone: A train of sharp pulses with a frequency of 1 Hz, width of 5 ms and amplitude of 0.75 mV, was presented to all of the units ($\forall i : V_i \rightarrow V_i + \Delta V$). The PS phased locked response is seen at the left half of the figure. At $t = 10$ sec, a tone of 0.75 mV was presented, by elevating the background input to the units across the network, resulting in the complete suppression of the PS response.

spontaneously or in response to external stimulation. This phenomenon opens up the possibility that some of the neuronal computations could be performed with the near coincident firing of neurons, but without an increase in the average discharge rate of neurons. Our analytical treatment of the network activity using the rate equations allowed us to better understand the dynamic mechanism of the PSs. In particular, it appears that sufficiently strong connections (or external inputs) induce a transition to a high rate saturated state of the network, which is then quickly terminated by synaptic depression. PSs therefore do not require direct synchronization of individual spikes (Mirralo and Strogartz, 1990; Hansel et al., 1995; van Vreeswijk et al., 1994). Whether direct synchronization plays any role in PS generation in network of spiking neurons (such as I&F) has to be studied more carefully. The dynamic mechanism of network synchronization described above is not very different from the one that causes population bursts in recently studied networks with spike-frequency adaptation (Latham et al., 2000; van Vreeswijk and Hansel, 2001). However, the bursts observed in these networks are much broader than the PSs studies here. We believe the difference is due to non-linear properties of the synaptic depression, which becomes faster for higher firing rates, and therefore quickly terminates the high-rate state. The way the networks with adaptation respond to external stimuli was not yet studied.

Importantly, for a given input the PS will or will not be generated depending on the state of depression for the synapses in the network at the time of the input. The response therefore depends on the previous history of the network activity, such as the previous inputs or on the particular distribution of the spontaneous activity across the network. This property raises an interesting possibility that the spontaneous activity in the brain does not merely represent a noise in the system, but in fact has an important functional role in information processing by shaping the responsiveness of the network to different stimuli. This possibility is most clearly demonstrated when considering the responses of the network to single excitatory pulses having various amplitude distributions across the network. The analytical calculations show that the response of the network to these pulses can be easily predicted. One should take a sum of the pulses amplitudes targeting every neuron in the network, where each amplitude is weighted by the depressing factor for synapses originated from this corresponding neuron, which in turn

depends on the spontaneous average rate of the neuron. The PS response will be generated if the computed sum exceeds the certain threshold. This resembles the simple perceptron rule, except that in our case the effective parameters of the 'perceptron' are fixed by the spontaneous activity, which therefore defines the computations performed by the network on its inputs.

Interestingly, our network generated the transient synchronization, characterized with single PS, even for constant step-like excitatory input. This resembles the transient response of single neurons in the primary auditory cortex responding to tonic stimulation. We found several other similarities between the behavior of our network with the known physiology of the auditory cortex, which we believe would be difficult to explain with other models. In particular, when applying periodic set of stimuli to the network, we observed that at low frequencies of stimulation the network could produce a PS response to every cycle of stimulation (perfect entrainment); however, when the frequency grows, some of the cycles are missed since the time between the stimuli is not enough for synapses to recover from depression. Surprisingly, above some cut-off frequency, the network can no longer generate the synchronization response, in accordance with the experimental observations in the auditory cortex (Kilgard and Merzenich, 1998). We also predict that under some circumstances, the cut-off frequency should have a non-monotonic dependency on the stimulus amplitude. Another nontrivial effect, which was observed in the auditory cortex and reproduced in the network, concerns the interference between simultaneously applied inputs of different nature. For example, a tonic stimulation that is applied on top of a periodic set of stimuli paradoxically prevents the network to respond to subsequent cycles of the periodic stimulus. This effect is also seen in the network, due to the increased depression of recurrent connections resulting from the tonic excitation.

Recent recordings from the auditory neurons demonstrated that some of them can be driven to rather high persistent activity (up to 40 Hz) by complex sounds (deCharms and Merzenich, 1998). It is not yet known whether such responses are synchronized across local populations of neurons. To try to account for the responses to complex time-dependent stimuli, we are planning to expand our network by including several iso-frequency columns. Future work will also include analyzing networks with combined excitatory and inhibitory circuits.

Appendix A

In this appendix we show how the equations for the steady state points and the equations for determining their stability can be derived. Starting from Eq. (9), taking into account the uniform distribution of the external inputs and taking the limit of large N , the following integral for $g_{st}(JH)$ is derived:

$$g(JH) = \frac{1}{N} \sum_{j=1}^N \frac{[JH + e_j]^+}{1 + \tau_{rec} U[JH + e_j]^+} \xrightarrow{N \rightarrow \infty} \frac{1}{\Delta e} \times \int_{e_1}^{e_N} \frac{[JH + e]^+}{1 + \tau_{rec} U[JH + e]^+} de \quad (A1)$$

which has the following solution ($\beta = \tau_{rec} U$):

$$0 \quad \text{If } JH < -e_N \quad (A2)$$

$$\frac{1}{\beta \Delta e} \left[e_N + JH - \frac{1}{\beta} \ln(1 + \beta(e_N + JH)) \right] \quad \text{If } -e_N \leq JH \leq -e_1 \quad (A3)$$

$$\frac{1}{\beta \Delta e} \left[\Delta e - \frac{1}{\beta} \ln \left(\frac{\beta(e_N + JH) + 1}{\beta(e_1 + JH) + 1} \right) \right] \quad \text{If } -e_1 \leq JH \quad (A4)$$

with which Eq. (8) can be solved. A unique non-trivial solution exists for (8) if $e_N > 0$, while up to 3 solutions exist (the 0 solution always one of them), depending on J , if $e_N < 0$. After finding H^* , planting it in (6a) and (6b) determine the steady state values of the network variables E^* & x^* . For determining the stability of the steady state found, we took advantage of the two distinct time scales of the network ($\tau_{rec} \approx 1$ sec, $\tau \approx 1$ ms) to make the approximation that immediately after a small perturbation is presented to a network lying in the steady state, the dynamics of the system is first governed by the dynamics of the rate variables (E_i 's). This leads to the following formulation:

$$H = \frac{1}{N} \sum_{i=1}^N E_i x_i^* \quad (A5)$$

$$\dot{H} = \frac{1}{N} \sum_{i=1}^N \dot{E}_i x_i^* \quad (A6)$$

Where E_i^* , x_i^* , H^* are as in Eqs. (6a–c). From Eqs. (1) and (A5) we get:

$$\tau \dot{E}_i = -E_i + \left[\frac{J}{N} \sum_{j=1}^N E_j x_j^* + e_i \right]^+$$

$$\begin{aligned} \Rightarrow \frac{\tau}{N} \sum_{i=1}^N \dot{E}_i x_i^* &= -\frac{1}{N} \sum_{i=1}^N E_i x_i^* \\ &+ \frac{1}{N} \sum_{i=1}^N \left[\frac{J}{N} \sum_{j=1}^N E_j x_j^* + e_i \right]^+ x_i^* \\ \Rightarrow \tau \dot{H} &= -H + \frac{1}{N} \sum_{j=1}^N \left[\frac{J}{N} \sum_{j=1}^N E_j x_j^* + e_i \right]^+ \\ &\times \frac{1}{1 + \beta E_i^*} \\ \Rightarrow \tau \dot{H} &= -H + \frac{1}{N} \sum_{i=1}^N \frac{[JH + e_i]^+}{1 + \beta[JH^* + e_i]^+} \\ &\equiv -H + \bar{g}(JH; H^*) \end{aligned} \quad (A7)$$

with the same assumptions as for (A1), the following integral is derived:

$$\bar{g}(JH; H^*) = \frac{1}{\Delta e} \int_{e_1}^{e_N} \frac{[JH + e]^+}{1 + \beta[JH^* + e]^+} de \quad (A8)$$

the solution of which is:

$$0 \quad \text{If } JH, JH^* < -e_N \quad (A9)$$

$$\frac{1}{\beta \Delta e} \left[e_N + JH - \frac{1 + \beta(JH^* - JH)}{\beta} \times \ln \left(\frac{1 + \beta(JH^* + e_N)}{1 + \beta(JH^* - JH)} \right) \right] \quad \text{If } -e_N < JH < JH^* < -e_1 \quad (A10)$$

$$\frac{1}{\Delta e} \left[\frac{(JH - JH^*)^2}{2} + \frac{1}{\beta} (e_N + JH^*) - \frac{1 + \beta(JH^* - JH)}{\beta^2} \ln(1 + \beta(JH^* + e_N)) \right] \quad \text{If } -e_N < JH^* < JH < -e_1 \quad (A11)$$

$$\frac{1}{\beta \Delta e} \left[\Delta e - \frac{1 + \beta(JH^* - JH)}{\beta} \times \ln \left(\frac{1 + \beta(JH^* + e_N)}{1 + \beta(JH^* + e_1)} \right) \right] \quad \text{If } -e_1 < JH, JH^* \quad (A12)$$

From (A2)–(A4) the value of the steady state (H^*) is calculated. Planting it at (A9)–(A12), and taking the derivative of the appropriate part of (A9)–(A12) at the steady state point, would yield its stability: if the derivative value is > 1 , the steady state is not stable, otherwise stable.

Appendix B

Transition from a stable steady state to a non-stable steady state is possible only when the curves of H & $\bar{g}(JH; H^*)$ have two intersection points. In the next two sections we give the constraints under which two intersection points can exist, and furthermore, when switching between stable and non-stable states can occur.

B.1. Dependency on the External Inputs

From theory and numerical analysis (confirmed by simulations), we have found that if:

$$0 \leq e_1 \leq e_N \quad (\text{B1})$$

(A2)–(A4) always give one solution to Eq. (8), H & $\bar{g}(JH; H^*)$ have only one intersection point (at the steady state of the system) for all values of J & β , and the steady state is always stable. If

$$e_1 \leq e_N \leq 0 \quad (\text{B2})$$

(A2)–(A4) can give either one (the 0 solution) or three different solutions to Eq. (8) (as a function of J & β , 0 always one of them). As for (B1), H & $\bar{g}(JH; H^*)$ have only one intersection point at the steady state H^* . While the 0 solution is always stable, the other two, if they exist, are not. Depending on the initial conditions, the network would either reach the 0 solution directly, or via a spontaneous PS. This result is due to the fact that now, unlike the case described in 3.1 (where only one steady state exists, with a value different than 0, resulting with an on going emergence of PSs), when the PS ends, the network enters the basin of attraction of the 0 solution, and no other spontaneous PS would occur.

The more interesting case is when:

$$e_1 \leq 0 \leq e_N \quad (\text{B3})$$

For which (A2)–(A4) always give one solution to Eq. (8), which is non-trivial, while H & $\bar{g}(JH; H^*)$ could have two intersection points, depending on the values of J & β . It is in this regime of the external inputs that transition can happen, and the network can switch between stable and non-stable states, as J is changed.

B.2. Dependency of J_c on β and the External Inputs

The curves of H & $\bar{g}(JH; H^*)$ can have two intersection points, depending on whether

$$\left. \frac{d\bar{g}(JH)}{d(JH)} \right|_{JH=-e_1} > \frac{1}{J} \quad (\text{B4})$$

This results from the fact that:

$$\left. \frac{d\bar{g}(JH)}{d(JH)} \right|_{JH>-e_1} = \text{Constant} \quad (\text{B5})$$

When condition (B4) is fulfilled, as in Fig. 2, as J increases, the intersection points of $\bar{g}(JH; H^*)$ & H can merge into one, and then separate again, the steady state of the network ‘jumps’ from the lower (stable) intersection point of $\bar{g}(JH; H^*)$ & H to the upper (unstable) one. The point of merging is the transition point, at which the network switches from stable state to spontaneous PSs activity. We are looking for an equation that will predict the value of J at that point.

We notice that at the merging point, the derivatives of the two branches of $\bar{g}(JH; H^*)$, (A10) and (A11), are equal, to each other and to the slope of H , which is $1/J$. Following this reasoning, we find that if:

$$\left. \frac{d\bar{g}(JH)}{d(JH)} \right|_{-e_N < JH^* < JH < -e_1, H=H^*} > \frac{1}{J} \quad (\text{B6})$$

the steady state is unstable, otherwise it is stable.

$$\begin{aligned} \Rightarrow \frac{1}{\beta \Delta e} \ln(1 + \beta(J_c H^* + e_N)) &= \frac{1}{J_c} \\ \Rightarrow J_c &= \frac{\beta \Delta e}{\ln(1 + \beta(J_c H^* + e_N))} \end{aligned} \quad (\text{B7})$$

Another demand is that $J_c H^* < -e_1$, which is derived from (B4). Solving (8) for the border condition of $g(JH^* = -e_1) = -e_1/J$:

$$\begin{aligned} (\text{A3}) \Rightarrow \frac{1}{\beta \Delta e} \left[\Delta e - \frac{1}{\beta} \ln(1 + \beta \Delta e) \right] &= \frac{|e_1|}{J_{e_1}} \\ \Rightarrow J_{e_1} &= \frac{|e_1| \beta \Delta e}{\Delta e - \frac{1}{\beta} \ln(1 + \beta \Delta e)} \end{aligned} \quad (\text{B8})$$

where J_{e_1} is the boundary value for which the steady state point is either in the $-e_N < JH^* < -e_1$ zone ($J < J_{e_1}$) or in the $-e_1 < JH^*$ zone ($J < J_{e_1}$). Only if $J_{e_1} > J_c$, transition could occur.

In simulations, for the chosen values of the parameters mentioned in 2.1, J_c was found to be ~ 4.1884 . The value of J_c obtained from the calculation above, for the same values of the parameters, was ~ 4.055 .

Appendix C

In this appendix we explain how a change in the external inputs can drive the network to switch into an unstable state:

Consider a network in a stable steady state. When introducing the network with an increase to the external inputs ($\forall i : e_i \rightarrow e_i + \Delta e, \Delta e > 0$), one can see from Eqs. (6a and b) that the new steady state satisfy the following relations: $E_{i-old}^* < E_{i-new}^* \Rightarrow x_{i-old}^* > x_{i-new}^*$. As $\tau \ll \tau_{rec}$ the change in $\{E_i\}_{i=1}^N$ will be much faster than the change in $\{x_i\}_{i=1}^N$, resulting in a situation, for Δe above some critical value and right after the onset of the stimulus, in which the new $\{E_{i-new}\}_{i=1}^N$, combined with the still high $\{x_{i-old}^*\}_{i=1}^N$, could drive the network to a PS. By following the above, the next equation for the dynamics of the mean-field variable right after the stimulus onset is derived:

$$\begin{aligned} \tau \dot{E}_i &= -E_i + \left[\frac{J}{N} \sum_{j=1}^N E_j x_{j-old}^* + e_{i-new} \right]^+ \\ &= -E_i + \left[\frac{J}{N} \sum_{j=1}^N E_j x_{j-old}^* + (e_{i-old} + \Delta e) \right]^+ \quad (C1) \\ \Rightarrow \tau \dot{H} &= -H + \frac{1}{N} \sum_{i=1}^N x_{i-old}^* [JH + (e_{i-old} + \Delta e)]^+ \\ &\equiv -H + \bar{g}_{new}(JH; H^*) \quad (C2) \\ \bar{g}_{new}(JH; H^*) &= \frac{1}{N} \sum_{i=1}^N \frac{[JH + (e_{i-old} + \Delta e)]^+}{1 + \tau_{rec} U[JH_{old}^* + e_{i-old}]} \\ &= \bar{g}(JH + \Delta e; H^*) \quad (C3) \end{aligned}$$

Figure 3d demonstrates an example of the formulation above, where the curve of (C3), which is identical to the curve of $\bar{g}(JH; H^*)$ with a shift to the left, was added to Fig. 2. We observe that immediately after the stimulus is presented (with an amplitude above the threshold), the graph of $\bar{g}_{new}(JH; H^*)$ no longer has intersection points with the graph of H , which means that there are no steady state points, hence the network activity will diverge to a PS.

If the input that was introduced to the network is a prolonged one, i.e. a tonic stimulus, after the PS the

network would recover itself to the new steady state values of $\{E_{i-new}^*\}_{i=1}^N$ & $\{x_{i-new}^*\}_{i=1}^N$ and no more PS would occur. If the input were a short one, i.e. a periodic stimulus, the network would recover to its original steady state values at the end of each phase of the stimulus.

Acknowledgments

We thank I. Nelken, N. Ulanovsky and L. Ahdut for fruitful discussions. We also wish to thank the anonymous reviewers for their helpful comments. This work was supported by grants from the Israeli Academy of Science, the office of Naval Research (USA), and the Edit C. Blair (New York) foundation.

References

- Abbott LF, Varela JA, Sen K, Nelson SB (1997) Synaptic depression and cortical gain control. *Science* 275: 220–224.
- Abeles M (1991) *Corticonics*. Cambridge University Press, New York.
- Abeles M, Prut Y (1996) Spatio-temporal firing patterns in the frontal cortex of behaving monkeys. *J. Physiol. Paris* 90(3/4): 249–250.
- deCharms RC, Blake DT, Merzenich MM (1998) Optimizing sounds features for cortical neurons. *Science* 280: 1439–1443.
- deCharms RC, Merzenich MM (1996) Primary cortical representation of sounds by the coordination of action-potential timing. *Nature* 381(6583): 610–613.
- Gray CM, König P, Engel AK, Singer W (1989) Oscillatory responses in visual cortex exhibit intercolumnar synchronization which reflects global stimulus properties. *Nature* 338: 334–337.
- Grossberg S (1988) *Nonlinear neural networks: Principles, mechanisms and architectures*. *Studies in Applied Mathematics* 52: 217–257.
- Hansel D, Mato G, Meunier C (1995) Synchrony in excitatory neural network. *Neural Comp.* 7: 307–337.
- Heil P (1997) Auditory cortical onset responses revisited. I. First-spike timing. *J. Neurophysiol.* 77(5): 2616–2641.
- Hopfield JJ (1995) Pattern recognition computation using action potential timing for stimulus representation. *Nature* 376: 33–36.
- Hubel DH, Wiesel TN (1962) Receptive fields, binocular interaction and functional architecture in the cat's visual cortex. *J. Physiol. (London)* 160: 106–154.
- Kilgard MP, Merzenich MM (1998) Plasticity of temporal information processing in the primary auditory cortex. *Nature Neuro.* 1: 727–731.
- Latham PE, Richmond BJ, Nelson PG, Nirenberg S (2000) Intrinsic dynamics in neuronal networks. *J. Neurophysiol.* 83: 808–827.
- Mirollo RE, Strogatz SH (1990) Synchronization of pulse-coupled biological oscillators. *SIAM J. Appl. Math.* 6: 1645–1647.
- Murphy JT, Kwan HC, Wong YC (1985) Cross-correlation studies in primate motor cortex: Synaptic interaction and shared input. *Can. J. Neurol. Sci.* 12: 11–23.
- Nelken I, Rotman Y, Bar-yosef O (1999) Responses of auditory-cortex neurons to structural features of natural sounds. *Nature* 397: 154–157.

- Phillips D, Sark S (1991) Separate mechanisms control spike numbers and inter-spike intervals in transient responses of cat auditory cortex neurons. *Hearing Research* 53: 17–27.
- Riehle A, Grun S, Diesman M, Aertsen A (1997) Spike synchronization and rate modulation differentially involved in motor cortical function. *Science* 278: 1950–1953.
- Rosenblatt F (1962) *Principles of Neurodynamics: Perceptrons and the Theory of Brain Mechanisms*. Spartan, Washington, DC.
- Singer W (1994) Coherence as an organizing principle of cortical functions. *Inter. Rev. Neuro.* 37: 153–183.
- Treves A (1993) Mean-field analysis of neuronal spike dynamics. *Network* 4: 259–284.
- Tsodyks M, Markram H (1997) The neural code between neocortical pyramidal neurons depends on neurotransmitter release probability. *PNAS* 94: 719–723.
- Tsodyks M, Pawelzik K, Markram H (1998) Neural networks with dynamic synapses. *Neural Computation* 10: 821–835.
- Tsodyks M, Uziel A, Markram H (2000) Synchrony generation in recurrent networks with frequency-dependent synapses. *J. Neurosci.* 20 RC1: 1–5.
- Tuckwell HC (1988) *Introduction to Theoretical Neurobiology*. Cambridge, UP, New York.
- Vaadia E, Aertsen A (1992) Coding and computation in the cortex: Single-neuron activity and cooperative phenomena. In: Aertsen, V Braitenberg, eds. *Information Processing in the Cortex*. Springer, Berlin, pp. 81–121.
- Vaadia E, Haalman I, Abeles M, Bergman H, Prut Y, Slovin H, Aertsen A (1995) Dynamics of neuronal interactions in monkey cortex in relation to behavioral events. *Nature* 373: 515–518.
- van Vreeswijk C, Abbott LF, Ermentrout GB (1994) When inhibition not excitation synchronizes neural firing. *J. Comput. Neurosci.* 1: 313–321.
- van Vreeswijk C, Hansel D (2001) Patterns of synchrony in neural networks with spike adaptation. *Neural Computation* 13: 959–992.
- Villa A, Tetko IV, Hyland B, Najem A (1999) Spatiotemporal activity patterns of rat cortical neurons predict responses in a conditioned task. *PNAS* 96: 1106–1111.
- Von der Malsburg C, Schneider W (1986) A neural cocktail-party processor. *bc* 54: 29–40.
- Wilson HR, Cowan JD (1972) Excitatory and inhibitory interactions in localized populations of model neurons. *Biophys. Journal* 12: 1–24.